

Understanding the energy scales relevant for the valence transition in YbInCu₄

I. Aviani, M. Očko, D. Starešinić, K. Biljaković, Alois Loidl, Joachim Hemberger, J. L. Sarrao

Angaben zur Veröffentlichung / Publication details:

Aviani, I., M. Očko, D. Starešinić, K. Biljaković, Alois Loidl, Joachim Hemberger, and J. L. Sarrao. 2009. "Understanding the energy scales relevant for the valence transition in YbInCu₄." *Physical Review B* 79 (16): 165112. <https://doi.org/10.1103/physrevb.79.165112>.



Understanding the energy scales relevant for the valence transition in YbInCu₄

I. Aviani,* M. Očko, D. Starešinić, and K. Biljaković
Institute of Physics, Bijenička cesta 46, P.O. Box 304, HR-10001 Zagreb, Croatia

A. Loidl and J. Hemberger
University of Augsburg, D-86135 Augsburg, Germany

J. L. Sarrao
Los Alamos National Laboratory, Los Alamos, New Mexico 87545, USA

(Received 3 December 2008; published 22 April 2009)

We report measurements and data analysis of specific heat, susceptibility, and transport properties of Yb_{0.5}Y_{0.5}InCu₄ in the temperature range between 2 and 300 K, and in magnetic fields of 0 and 5 T. The data can be consistently explained within the local-moment crystal-field theory with two close-lying doublets, Γ_6 and Γ_7 , in the ground state and a Γ_8 excited quartet, and with very weak or even absent Kondo effect. The crystal-field scheme proposed by this work, which differs from the one widely accepted in the literature, provides a better understanding of the relevant energy scales and the valence transition in the YbInCu₄.

DOI: [10.1103/PhysRevB.79.165112](https://doi.org/10.1103/PhysRevB.79.165112)

PACS number(s): 75.30.Mb, 71.27.+a, 75.20.Hr, 71.70.Ch

I. INTRODUCTION

The intermetallic compound YbInCu₄ is one of the most intriguing rare-earth compounds exhibiting a very rare, still not well understood, valence phase transition which is interesting from both technological and fundamental aspects. A large magnetic entropy change at the transition could be used in thermomagnetic devices. In addition, the transition temperature can be tuned by doping. Knowing the relevant energy scales is crucial for understanding and modeling the transition. The first-order isostructural valence transition at $T_V=42$ K (Ref. 1) is characterized by the change in the valence and the magnetic character of Yb³⁺ ion. The high-temperature local-moment (LM) phase, is semimetallic and paramagnetic with the magnetic moment 5%–10% lower than the Yb³⁺ free-ion value. The low-temperature valence fluctuating (VF) phase is a nonmagnetic heavy fermion state.^{2,3} At the transition the holes, originally located on an ytterbium ion, delocalize into the conducting band.¹ According to recent hard-x-ray PES (photoemission spectra) data, the Yb valence decreases from 2.9 to 2.74.⁴ The decrease is accompanied by an order of magnitude increase in conductivity and by a 0.5% lattice expansion. It is widely accepted that the Kondo temperature changes from approximately $T_K^{LM}=25$ K in the LM phase to $T_K^{VF}=400$ K in the VF phase.⁵ To elucidate this transition different experiments have been performed on YbInCu₄ and related compounds.^{2,6–8} The phase diagrams have been studied by doping, applying hydrostatic pressure and external magnetic fields.

Different theoretical models have been used to describe the experimental results.^{9,10} The reduction in the Yb moment in the LM phase indicates the existence of an interaction between itinerant d and localized f electrons. It is important to find out more about this interaction because it is responsible for the onset of the transition. Two different assumptions are found in the literature: (i) the f - d interaction is the Kondo exchange and (ii) the f - d interaction is the Falicov-Kimball (FK) Coulomb repulsion.¹⁰ The FK interaction suc-

cessfully explains the moment reduction in terms of delocalization of holes. It also explains the main features of the LM phase and the transition but gives a too large valence change (close to 1). In the case of the Kondo interaction, $T_K^{LM}=25$ K is needed to explain the moment reduction.² Although this value is commonly accepted in the literature there is not much evidence for the Kondo effect in the LM phase. Besides the magnetic susceptibility data,² the evidence is based on neutron-scattering data, showing an inelastic absorption maximum at 2.3 meV which is attributed to Kondo scattering.⁵ Recently a broad maximum at 10 K in specific heat in pressure-stabilized LM phase was interpreted in terms of the Kondo effect.¹¹ On the other hand it is widely accepted that the position of the inelastic neutron absorption maximum is actually at 3.8 meV and that it reflects scattering from the CF (crystal field) levels^{12,13} rather than Kondo scattering. There are a number of indications that the Kondo effect in the LM phase is weak or even absent. The value of $T_K^{LM}=25$ K is rather large and difficult to reconcile with the semimetallic character of the LM phase. The paramagnetic Curie-Weiss temperature, which is expected to be of the order of T_K^{LM} , is only a few Kelvin and can be attributed to the CF effects. A logarithmic term in the resistance is absent, the magnetoresistance is weak, and the Hall constant is typical for semimetals. For details see the discussion in Ref. 10. Finally, the Kondo volume collapse model⁹ does not seem to describe the transition because the volume change is too small.

The magnetic phase diagram is successfully explained simply by taking into account the Yb³⁺-ion magnetic entropy change.¹⁴ This clearly demonstrates the importance of the magnetic degrees of freedom. The energy-level scheme for the Yb³⁺ ion obtained from neutron inelastic scattering in the LM phase of YbInCu₄ (Ref. 12) is shown in Fig. 1. The overall CF splitting $T_{CF}=44$ K is consistent with the entropy change at the transition,² but a more precise determination of the CF scheme was not possible because the valence transition sets in at $T_V=42$ K, very close to T_{CF} , making the LM phase inaccessible at lower temperatures. For the same rea-

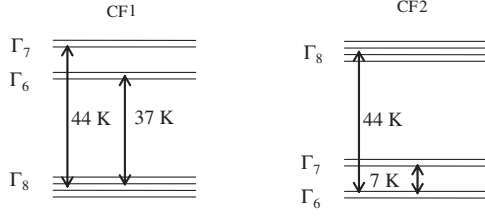


FIG. 1. The CF schemes for the Yb^{3+} ion in the cubic environment of YbInCu_4 . The CF1 scheme is proposed from the results of inelastic neutron scattering (Ref. 12) and widely accepted in literature. The CF2 scheme is proposed by this work. For both schemes the total CF splitting $T_{\text{CF}} \equiv \Delta_2 = 44$ K is an order of magnitude greater than spacing between the doublets $\Delta_1 = 7$ K. The system can be considered as a system of two quartets, with one of them being composed of two closely spaced Kramers doublets. For temperatures larger than the doublet splitting, $T \gg \Delta_1$, the system behaves like two quartets with total CF spacing Δ_2 and it is not possible to distinguish between the two schemes.

son T_K^{LM} could not be estimated more accurately. As the relevant energy scales T_V , T_{CF} , and T_K^{LM} are nearly equal, we found it necessary to lower T_V , i.e., to extend the LM phase down to lower temperatures, in order to separate T_{CF} and T_K^{LM} . This can be done by applying a hydrostatic pressure, magnetic field, or by doping.

Hydrostatic pressure stabilizes the LM phase down to very low temperatures. In that case, the magnetic entropy is released by ferromagnetic ordering of uncompensated Yb^{3+} moments. The pressure-induced small-moment ferromagnetism is found in magnetization measurements of $\text{Yb}_{0.8}\text{Y}_{0.2}\text{InCu}_4$,¹⁵ in resistivity and ac susceptibility,¹⁶ and in the specific heat¹¹ of YbInCu_4 . The corresponding pressure-temperature phase diagram has been extensively studied recently.¹⁷ The specific-heat data¹¹ exhibit a broad maximum around 10 K which is attributed to the combination of Kondo and CF effects.

The LM phase is also stabilized by yttrium doping in $\text{Yb}_x\text{Y}_{1-x}\text{InCu}_4$. For concentrations $x < 0.8$ the valence transition is completely suppressed.¹⁸ The measured anisotropic high-field magnetization and the magnetic phase diagram obtained on a single crystal of YbInCu_4 (Ref. 19) is explained with the CF1 scheme from Ref. 12 (see Fig. 1). However, the low-field low-temperature magnetization data in the LM phase of a single crystal of $\text{Yb}_{0.7}\text{Y}_{0.3}\text{InCu}_4$ (Ref. 19) exhibits anisotropy that is not expected within the proposed CF scheme.

Our previous investigations of the LM phase of $\text{Yb}_x\text{Y}_{1-x}\text{InCu}_4$ showed that the temperature of the thermopower minima does not change by doping and also that magnetic susceptibilities scale with concentration of Yb^{3+} ions down to 2 K.^{18,20} This indicates that the CF levels and the magnetic properties of the Yb ion do not change by doping and that the Y-doped sample is relevant for studying the LM phase at low temperatures. In this paper we report measurements and data analysis of specific heat, magnetic susceptibility, electrical resistance, and thermopower of $\text{Yb}_{0.5}\text{Y}_{0.5}\text{InCu}_4$ in the temperature range between 2 and 300 K.

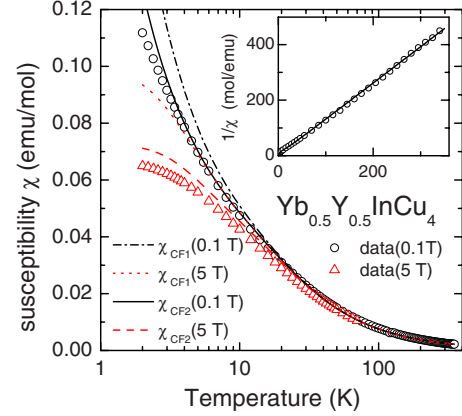


FIG. 2. (Color online) Magnetic susceptibility of $\text{Yb}_{0.5}\text{Y}_{0.5}\text{InCu}_4$ as a function of temperature measured in magnetic fields of 0.1 T (circles) and 5 T (triangles). The dashed-dotted and the dotted lines are the calculated susceptibilities for the CF1 scheme in magnetic fields of 0.1 and 5 T, respectively. The full and the dashed lines are the calculated susceptibilities for the CF2 scheme in magnetic field of 0.1 and 5 T, respectively. The corresponding Curie-Weiss plot for 0.1 T is shown in the inset where the full line is the calculated inverse susceptibility.

II. RESULTS AND DISCUSSION

The most convenient concentration we found is for $\text{Yb}_{0.5}\text{Y}_{0.5}\text{InCu}_4$: it is concentrated enough to obtain a strong response of Yb ions and dilute enough to avoid possible coherence effects. The measurements were performed on single crystals grown in In-Cu flux.²¹ The experimental data are obtained on samples from the same batch. Quantum design's physical property measurement system (PPMS) was used to measure dc magnetic susceptibility and specific heat. The transport properties were measured as described in Ref. 18. The susceptibility data obtained for magnetic fields of 0.1 and 5 T are shown in Fig. 2. The Curie-type susceptibility, shown in the inset, shows that the sample is in the LM phase down to 2 K. The slope of the inverse susceptibility corresponds to the concentration $x^{3+} = 0.315$ of magnetic Yb^{3+} free ions. This value is used to scale the magnetic contribution for all theoretical curves in this work. The concentration x^{3+} is lower than the nominal one $x = 0.5$ so that the rest of ytterbium ions are considered to be nonmagnetic Yb^{2+} ions.¹⁸ The magnetic contribution of the Yb^{3+} CF levels is calculated for the two different CF schemes from Fig. 1 by exact diagonalization of the CF Hamiltonian of Yb^{3+} ion ($j = 7/2$) in a cubic CF in an external magnetic field. The data calculated for the CF2 scheme are in much better agreement with the experimental results (see Fig. 2).

The low-temperature specific-heat data divided by temperature c_p/T for $\text{Yb}_{0.5}\text{Y}_{0.5}\text{InCu}_4$ measured in zero magnetic field and in a field of 5 T are shown in Fig. 3 along with the theoretical curves, consisting of a sum of nonmagnetic and magnetic contributions. The nonmagnetic part is assumed to be equal to the measured specific heat c_0/T of nonmagnetic isostructural and isoelectronic YInCu_4 .²² The magnetic contribution is calculated from the CF Hamiltonian and scaled by the concentration factor x^{3+} . The data calculated for a

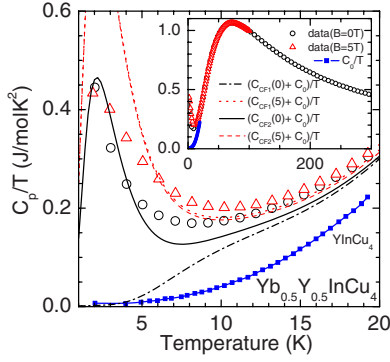


FIG. 3. (Color online) Low-temperature specific heat of $\text{Yb}_{0.5}\text{Y}_{0.5}\text{InCu}_4$ divided by temperature as a function of temperature in zero magnetic field (circles) and in a magnetic field of 5 T (triangles). The data in the whole temperature range are shown in the inset. The squares are the specific-heat data of nonmagnetic YInCu_4 from Ref. 22. Note the upturn in c_p/T at low temperatures. Theoretical values for the two CF schemes and for the fields of 0 T and 5 T are also shown in the figure for a comparison.

magnetic field of 5 T show a very similar behavior for the both CF schemes (the dotted line and the dashed line which overlap), while for the zero magnetic field (dash-dotted line and the full line) the behavior for the two schemes differs completely. The CF1 scheme fails to explain the upturn in c_p/T obtained at low temperatures. The upturn could be attributed to the Kondo effect, with the T_K of only few K. For the CF2 scheme the upturn is easily explained within the simple CF theory as the result of the occupation of the two close-lying ground-state doublets.

Magnetic entropies of the Yb^{3+} ion in $\text{Yb}_{0.5}\text{Y}_{0.5}\text{InCu}_4$ as function of temperature are shown in Fig. 4. The data are obtained by integrating the difference $(c_{\text{mag}}/T - c_0/T)$ from Fig. 3. They are scaled for the concentration of Y^{3+} ions and then shifted to match the high-temperature theoretical CF curves. The lines are the calculated entropies for the two CF schemes. For temperatures larger than the doublet separation, $T \gg \Delta_1$, the doublet splitting can be neglected and the system behaves like a system of two simple quartets with total CF spacing equal Δ_2 . Therefore for temperatures above 20 K the

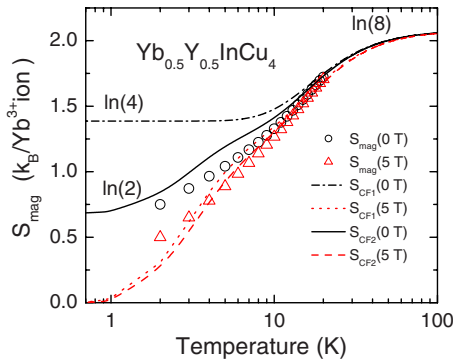


FIG. 4. (Color online) Symbols show the magnetic entropy obtained in magnetic fields of 0 T (circles) and 5 T (triangles). The lines are the calculated entropies for the Yb^{3+} ion for CF1 (dashed-dotted line for 0 T and dotted line for 5 T) and for CF2 (full line for 0 T and dashed line for 5 T).

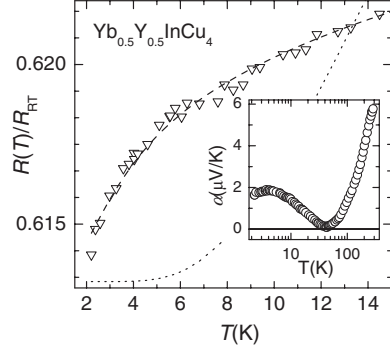


FIG. 5. The transport data of $\text{Yb}_{0.5}\text{Y}_{0.5}\text{InCu}_4$ as function of temperature. Triangles are the low-temperature resistivity data, measured with respect to the room-temperature value. The dashed line is the fit to the CF2 contribution, and the dotted line for the CF1 contribution (see text). The circles in the inset are the thermopower data.

results do not differ for the two schemes. At high temperatures all eight CF levels are equally occupied, and the magnetic entropy assumes the maximum value of $k_B \ln(8)$. A significant difference in residual entropies is expected for the two schemes because of the different degeneracies of their ground states: $k_B \ln(4)$ for the quartet and $k_B \ln(2)$ the doublet ground state, respectively. Figure 4 shows that, at low temperatures, the measured zero-field magnetic entropy is in good agreement with theoretical data for the doublet ground state. The Zeeman energy splits the ground-state multiplet leading to a singlet ground state and the residual entropy falls to zero. This behavior is observed for the data measured in the magnetic field of 5 T. The analysis shows that the CF2 scheme explains the experimental results much better than the CF1 scheme.

The transport data for $\text{Yb}_{0.5}\text{Y}_{0.5}\text{InCu}_4$ as function of temperature are shown in Fig. 5. The resistivity shows no sign of the Kondo effect, i.e., no characteristic low-temperature upturn. Moreover, the resistance decreases down to the lowest temperatures. The decrease cannot be ascribed to the onset of coherence which is not expected for a diluted ($x=0.5$) sample. We believe that the temperature dependence of the resistance reflects the scattering on the localized Yb^{3+} -ion $4f$ levels, split by the CF. The dashed line represents a fit to Hirst's formula,²³ $R(T) = R_0 + \sum_i (a_i \Delta_i / T) / [\exp(\Delta_i / T) - 1]$, which describes the resistivity arising from the scattering by CF levels. The CF energy levels are taken to be $\Delta_1 = 7$ K and $\Delta_2 = 44$ K, which correspond to the CF2 scheme, while the R_0 and a_i are the fitting parameters. A discussion of parameters is given in Ref. 24 and references therein. For a comparison the best fit for the CF1 scheme is also shown by the dotted line. The thermopower exhibits a minimum at 44 K and a maximum at 5 K. We think that both extrema indicate scattering on CF levels; the minimum scattering on the excited quartet and the maximum scattering on the first excited CF doublet.

We find our data, presented in this work, are relevant to estimate the CF energy scheme and the strength of the Kondo interaction in the LM phase of the YbInCu_4 . The low-temperature anomalies obtained in the LM phase can be explained with the CF2 scheme, shown in Fig. 1, and a small

or even absent Kondo energy. It is important to note that the CF2 scheme proposed in this work is not in contradiction with the neutron-scattering data^{12,13} which only show one inelastic absorption peak corresponding to the overall CF splitting. This is in accord with the picture in which E_F is placed just below the dip in the density of states (DOS). Large electrical resistance of the LM phase and its increase when a noninteger valence Yb is substituted by trivalent Y,¹⁸ forcing a hole localization, support this picture. Our results support the FK scenario for the onset of the valence transition in YbInCu₄. At the transition hole delocalization pushes E_F deeper in the DOS where the density of states is higher. This sets up the Kondo interaction (with high characteristic temperature $T_K^{\text{VF}}=400$ K) which screens Yb moments. A new equilibrium itinerant hole concentration (and Yb valence) is fixed by the equilibrium between the Kondo condensation energy gain and the magnetic entropy lost due to the quenching of the Yb³⁺ moments. The VF phase is stabilized when about 15% of holes are delocalized. In other words, T_V depends on FK parameters and the valence change depends on the T_K^{VF} of the VF phase. In the simplest picture, we assume the Kondo condensation energy E_K is proportional to the product of the concentration x^{3+} of the Yb³⁺ ions and the concentration of delocalized itinerant holes $1-x^{3+}$, $E_K=T_K^{\text{VF}}x^{3+}(1-x^{3+})$. If we neglect the entropy of the Fermi liquid, the entropy change at the transition is roughly

$T_V x^{3+} \ln(4)$. By equating these two expressions we obtain the valence change at the transition $1-x^{3+}=T_V \ln(4)/T_K^{\text{VF}}=42 \text{ K} \ln(4)/400 \text{ K}=0.15$ that is the experimentally observed value.

III. CONCLUSIONS

We present measurements and data analysis of specific heat, magnetic susceptibility, electrical resistance, and thermopower of Yb_{0.5}Y_{0.5}InCu₄. Our measurements show that the low-temperature properties of the local-moment phase of YbInCu₄ can be explained only by the CF effects but with a modified CF scheme. The data are consistently explained with two close-lying doublets, Γ_6 and Γ_7 , in the ground state and a Γ_8 excited quartet. This also implies that the Kondo interaction in this system is very weak. We find our results relevant for a better understanding of the valence transition, as well as of the low-temperature properties of the pressure stabilized LM phase of YbInCu₄.

ACKNOWLEDGMENTS

This work was supported by the Croatian Ministry of Science, Education and Sports Project No. 035-0352827-2841 and the ECOM COST Action P16.

*aviani@ifs.hr

- ¹I. Felner and I. Nowik, Phys. Rev. B **33** 617 (1986); I. Felner, I. Nowik, D. Vaknin, U. Potzel, J. Moser, G. M. Kalvius, G. Wortmann, G. Schmiester, G. Hilscher, E. Gratz, C. Schmitzer, N. Pillmayr, K. G. Prasad, H. de Waard, and H. Pinto, *ibid.* **35** 6956 (1987); I. Nowik, I. Felner, J. Voiron, J. Beille, A. Najib, E. du Tremolet de Lacheisserie, and G. Gratz, *ibid.* **37**, 5633 (1988).
- ²J. L. Sarrao, C. D. Immer, C. L. Benton, Z. Fisk, J. M. Lawrence, D. Mandrus, and J. D. Thompson, Phys. Rev. B **54**, 12207 (1996).
- ³J. L. Sarrao, A. P. Ramirez, T. W. Darling, F. Freibert, A. Migliori, C. D. Immer, Z. Fisk, and Y. Uwatoko, Phys. Rev. B **58**, 409 (1998).
- ⁴H. Sato, K. Shimada, M. Arita, K. Hiraoka, K. Kojima, Y. Takeda, K. Yoshikawa, M. Sawada, M. Nakatake, H. Namatame, M. Taniguchi, Y. Takata, E. Ikenaga, S. Shin, K. Kobayashi, K. Tamasaku, Y. Nishino, D. Miwa, M. Yabashi, and T. Ishikawa, Phys. Rev. Lett. **93**, 246404 (2004).
- ⁵J. M. Lawrence, S. M. Shapiro, J. L. Sarrao, and Z. Fisk, Phys. Rev. B **55**, 14467 (1997).
- ⁶C. D. Immer, J. L. Sarrao, Z. Fisk, A. Lacerda, C. Mielke, and J. D. Thompson, Phys. Rev. B **56**, 71 (1997).
- ⁷T. Koyama, M. Matsumoto, T. Tanaka, H. Ishida, T. Mito, S. Wada, and J. L. Sarrao, Phys. Rev. B **66**, 014420 (2002).
- ⁸V. Fritsch, J. D. Thompson, S. Bobev, and J. L. Sarrao, Phys. Rev. B **73**, 214448 (2006).
- ⁹J. W. Allen and R. M. Martin, Phys. Rev. Lett. **49**, 1106 (1982); J. W. Allen and L. Z. Liu, Phys. Rev. B **46**, 5047 (1992).

- ¹⁰J. K. Freericks and V. Zlatić, Rev. Mod. Phys. **75**, 1333 (2003).
- ¹¹T. Park, V. A. Sidorov, J. L. Sarrao, and J. D. Thompson, Phys. Rev. Lett. **96**, 046405 (2006).
- ¹²A. Severing, E. Gratz, B. D. Rainford, and K. Yoshimura, Physica B **163**, 409 (1990).
- ¹³A. P. Murani, D. Richard, and R. Bewley, Physica B **312-313**, 346 (2002).
- ¹⁴M. O. Dzero, L. P. Gor'kov, and A. K. Zvezdin, J. Phys.: Condens. Matter **12**, L711 (2000).
- ¹⁵A. Mitsuda, T. Goto, K. Yoshimura, W. Zhang, N. Sato, K. Kosuge, and H. Wada, Phys. Rev. Lett. **88**, 137204 (2002).
- ¹⁶T. Mito, T. Koyama, M. Shimoide, S. Wada, T. Muramatsu, T. C. Kobayashi, and J. L. Sarrao, Phys. Rev. B **67**, 224409 (2003).
- ¹⁷T. Mito, M. Nakamura, M. Otani, T. Koyama, S. Wada, M. Ishizuka, M. K. Forthaus, R. Lengsdorf, M. M. Abd-Elmeguid, and J. L. Sarrao, Phys. Rev. B **75**, 134401 (2007).
- ¹⁸M. Očko, J. L. Sarrao, I. Aviani, Dj. Drobac, I. Živković, and M. Prester, Phys. Rev. B **68**, 075102 (2003); M. Očko and J. L. Sarrao, Physica B **312-313**, 341 (2002).
- ¹⁹N. V. Mushnikov, T. Goto, E. V. Rozenfeld, K. Yoshimura, W. Zhang, M. Yamada, and H. Kageyama, J. Phys.: Condens. Matter **15**, 2811 (2003).
- ²⁰I. Aviani, (unpublished).
- ²¹J. L. Sarrao, Physica B **259-261**, 128 (1999).
- ²²H. Nakamura, K. Ito, A. Uenishi, H. Wada, and M. Shiga, J. Phys. Soc. Jpn. **62**, 1446 (1993).
- ²³L. L. Hirst, Solid State Commun. **5**, 751 (1967).
- ²⁴M. Očko, J.-G. Park, I. Aviani, Physica B **259-261**, 260 (1999).